

DOI: 10.5281/zenodo.4465494

# MULTIANALYTICAL TECHNIQUES OF AL-BĪMĀRISTĀN AL-MU'AYYIDI MURAL PAINTING AT HISTORIC CAIRO: CONTRIBUTION TO CONSERVATION AND RESTORATION

Mona F. Ali<sup>1</sup>, Hazem El-Shafey<sup>2</sup> and Hussein Marey Mahmoud\*<sup>1</sup>

<sup>1</sup>Department of Conservation, Faculty of Archaeology, Cairo University, 12613 Giza, Egypt

<sup>2</sup>Conservator, Master student, Department of Conservation, Faculty of Archaeology, Cairo University, Egypt

Received: 24/12/2020

Accepted: 20/01/2021

\*Corresponding author: H. Marey Mahmoud (marai79@hotmail.com)

## ABSTRACT

In the present study, rare Islamic mural painting of Al-Bimāristān Al-Mu'ayyidi (1418/1420 AD & 821/823 AH) at historic Cairo has been uncovered and studied. A number of analytical methods included hand-held digital optical microscope, polarized light microscope (PLM), field-emission scanning electron microscope with energy dispersive X-ray analyzer (FE-SEM/EDAX), X-ray diffraction analysis (XRD) and Fourier-transform infrared analysis (FTIR) were useful to characterize some painted fragments. The results allowed to differentiate the stone as bioclastic-type limestone and its mineralogical composition as calcite ( $\text{CaCO}_3$ ) and halite ( $\text{NaCl}$ ). The render layer was made of calcite with few amounts of quartz ( $\text{SiO}_2$ ). Individual pigment minerals such as lazurite 'Lapis Lazuli' ( $(\text{Na, Ca})_8(\text{AlSiO}_4)_6(\text{SO}_4, \text{S, Cl})_2$ ) for the blue color and red lead 'Minium' ( $\text{Pb}_3\text{O}_4$ ) for the orange-red color, were identified. A mixture combined azurite ( $\text{Cu}_3(\text{CO}_3)_2(\text{OH})_2$ ) and yellow orpiment ( $\text{As}_2\text{S}_3$ ) was used to produce the green color, while hematite ( $\text{Fe}_2\text{O}_3$ ), gypsum ( $\text{CaSO}_4 \cdot 2\text{H}_2\text{O}$ ) and calcite were used for the pink hue. Further, 'fresco' was confirmed as a painting technique. The studied mural and the entire building showed a serious state of conservation. The deterioration factors included environmental impacts (earthquakes, groundwater) and anthropogenic ones. The aspects were in form of structural damage of the architectural elements, several cracks, salt efflorescence and disfiguration of the painted surfaces. Based on these inputs, a restoration project was a priority to eliminate the deterioration process and to stabilize the preservation state of the studied mural.

---

**KEYWORDS:** Historic Cairo, Mural painting, XRD, FE-SEM/EDX, FTIR, Lapis lazuli, Fresco, Restoration

---

## 1. INTRODUCTION

Bimāristān is derived from the Persian word to mean hospital. Al-Bimāristān Al-Mu'ayyidi (Figs. 1& 2) (under registration number: 257) was built by Sultan Al-Mu'ayyad between 1418 and 1420 AD (821-823 AH) (Holt, 1993; Behrens-Abouseif, 2007). It was the second public hospital built in Cairo after that of Qalawun at 1284 AD (682 AH) (Abdel Alim, 2003). It is noted for its monumental scale, unprecedented in a civic building, which was clearly inspired by the nearby free-standing grandiose Madrasa of Sultan Hassan, and also for its portal, which is set in a pishtaq, a feature which gives the facade a Persian character. The portal has a Muqarnas hood and a window with a pair of colonnettes with a snake, a symbol of healing. The Bimāristān is built on the site of the Madrasa of Sultan al-Ashraf Sha'ban, which was

founded in 1375 AD (776 AH) and demolished by Sultan Farag ibn Barquq in 1411 AD (813 AH). The building has lost many sections of its outlying structure. The area in front was leveled in 2005 by the Supreme Council of Antiquities to allow a full view of the Maristan's facade. Some of the surviving remains of the Bimāristān are: a) the main façade, b) the entrance block, c) a vestibule (dihliz), a mosque, and large courtyard surrounded by four Iwans (Hampikian, 2012). Since 1928, the monument was a subject for many restoration interventions for reinforcing its architectural elements. Restoration of the entrance and main facade was performed in 1939 by the Committee for the Conservation of the Monuments of Arab Art. Also, the committee enlarged its surrounding area by removing many nearby houses. In 1957, the western court was restored, and a recent house that illegally was built on it was removed.

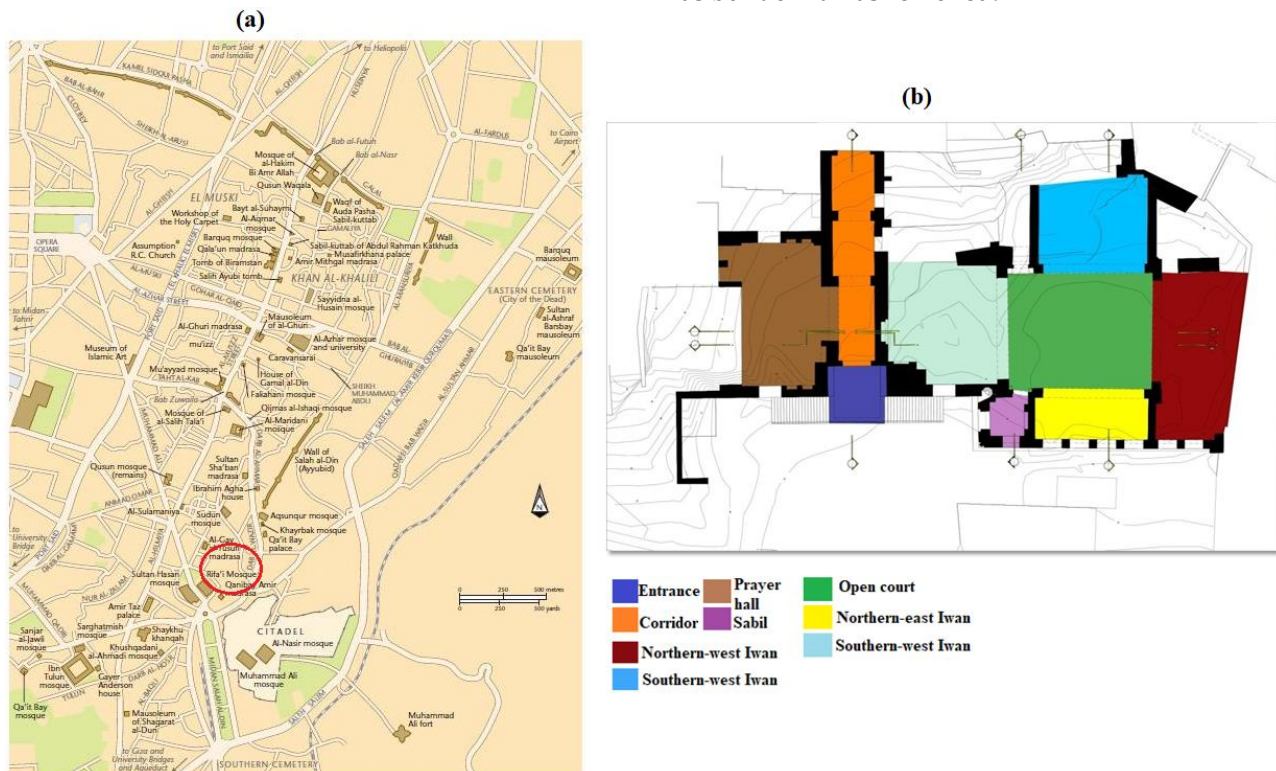


Figure 1. a) map of historic Cairo (after: Yeomans, 2006), the location of Al-Bimāristān Al-Mu'ayyidi complex is highlighted by red circle, b) a schematic plan of the buildings complex.

Compared with other art styles, mural paintings were not a favorite technique for Islamic buildings and few examples were documented. For these rare cases, regrettably countable studies have been undertaken. The murals of Qusayr Amra dated to 750 AD (132 AH) in Jordan were analyzed and pigments of green earth, yellow ochre ( $\alpha$ -FeOOH), red ochre ( $\alpha$ -Fe<sub>2</sub>O<sub>3</sub>), realgar (As<sub>4</sub>S<sub>4</sub>), bone black and lapis lazuli [(Na,Ca)<sub>8</sub>Al<sub>6</sub>Si<sub>6</sub>O<sub>24</sub>(S,SO)<sub>4</sub>] were found (Bianchin et al., 2007). In their study of wall paintings from the 11th-12th centuries of al-Qarawiyyin Mosque in Fez,

Morocco, Fikri et al., (2018) identified red ochre, calcite (CaCO<sub>3</sub>), copper pigments (azurite, Cu<sub>3</sub>(CO<sub>3</sub>)<sub>2</sub>(OH)<sub>2</sub>), cinnabar ( $\alpha$ -HgS), and lead pigments. Also, Arab mural paintings (dated back to the 10th-11th centuries) from the Cercadilla archaeological site in Spain were examined by analytical means such as Wavelength Dispersive X-ray fluorescence (WD-XRF), FTIR and micro X-ray diffraction analysis ( $\mu$ -XRD) (Gil-Torrano et al., 2019).

In a recent research, Ali and Abd Elkawy (2021) applied a scientific restoration intervention for the paint layers of Taqi Al-Din El-Bistami's hospice at Cairo, its

date goes back to 1443 AD (874 AH). They concluded that the murals have been executed by the tempera

technique using pigments of hematite, cinnabar, malachite ( $\text{Cu}_2(\text{CO}_3)(\text{OH})_2$ ), goethite and ultramarine blue.



Figure 2. Left: the entrance unit of Al-Bīmāristān Al-Mu'ayyidi, before restoration; right: location of the surviving mural painting (highlighted with arrow) before complete uncovering and restoration.

For a number of decades, multi physical and chemical methods were used to study heritage materials. It is useful to identify the composition of the materials to evaluate their artistic and technological values and to understand their degradation mechanisms. Since few examples for the Islamic mural paintings are known, the present study fulfills a notable target to address some requirements as follows:

- to characterize the paint layers used to create the mural in the studied building, using multianalytical methods, and to compare the results with examples from the same historical period,
- to assess the deterioration factors and forms, and
- to apply a restoration project to minimize the occurred damage.

## 2. MATERIALS AND METHODS

### 2.1. Samples

Tiny samples of stone, render and paint layers were collected. The pigment samples included colors of blue, orange, green, pink and black.

### 2.2. Digital microscope

Stereomicroscopic examination on the studied samples was applied using a Zeiss Microscope Leica M 715a. The microscopic images helped in understanding the hue appearance of the paint layers, their

stratigraphic order, the size of particles and their distribution in the matrix.

### 2.3. Polarized light microscope

Thin-sections on stone and render samples were prepared to identify their petrographic composition. The petrographic examination reflects many microscopic features which help to define the stone type and also to describe the main minerals used in the render layer. The sections were analyzed using a Nikon Eclipse E600 Microscope conducted with Nikon Cooplix camera 990.

### 2.4. Field-emission scanning electron microscope

This microscope is widely used to describe the morphological features of paint layers, and it gives good results in the absence of organic binders (Goldstein et al., 2007). The morphological profile of each sample was determined through a Quanta 250 Scanning Electron Microscope. The investigations were performed at accelerating voltage of 20-25 kV. The microanalysis of samples was detected by an energy-dispersive X-ray analyzer (EDAX).

### 2.5. X-ray diffraction analysis

The X-ray diffraction patterns of the powder samples were collected using a Philips PW 1840d XRD diffractometer. The instrument was operated at a power of 40 kV using a Cu-K $\alpha$  radiation wavelength

of 1.54053 Å and generator current of 25 mA. Mineral phase interpretations were accessed by a match3 software.

### 2.6. Fourier-transform infrared spectroscopy

FTIR analysis was made by BruKER Vertex 70 spectrometer. Spectra were recorded at the region (400–4000  $\text{cm}^{-1}$ ), on KBr pellets with a resolution of 4  $\text{cm}^{-1}$ . The spectra are usually analyzed and matched with standard materials in the FTIR library.

## 3. RESULTS AND DISCUSSION

The results obtained following the application of multianalytical techniques on samples of stone, render and paint layers are presented in this section. Further, the interpretations of results were compared with previous studies on similar objects. Table 1 shows the EDAX microanalysis of the studied samples.

### 3.1. Stone support

Samples of the stone support were collected and studied. Understanding the mineralogical-chemical composition of the support helps in determining, in somehow, the deterioration mechanisms of the whole mural. The petrographic study on thin-sections of stone samples shows clearly a bioclastic-type limestone which contains several large-size fossils. The background of the section is filled with a micritic texture (Mahmoud, 2021). New formed fine calcite crystals were deposited into the cytoplasmic structure of fossils (Fig. 3a). Scanning electron microscope was used to identify the morphological aspects of stone samples. In Figure 4a, the FE-SEM investigation shows fine and large grains distributed into the micrograph.

Table I. EDAX analysis of the studied samples shows the contained elements

Element	Stone	Render	Blue pigment	Orange pigment	Green pigment	Pink pigment
C	4.01	4.93	5.37	6.43	6.98	5.85
O	51.31	52.23	55.09	36.66	49.34	52.40
Na	0.44	0.69	0.58	-	-	-
Mg	-	0.08	0.01	-	-	-
Al	0.05	0.01	0.76	-	-	-
Si	0.62	0.42	0.79	1.18	0.54	1.93
S	0.15	2.85	6.06	-	5.47	5.12
Cl	1.20	1.60	0.80	3.74	1.21	0.56
K	0.51	-	-	-	-	-
Ca	41.51	37.18	29.97	27.59	24.71	31.00
Ba	-	-	-	-	2.05	-
Fe	0.20	-	0.20	-	-	3.14
Cu	-	-	-	-	3.88	-
As	-	-	-	-	5.83	-
Pb	-	-	-	24.40	-	-

The EDAX spectrum of the sample (Fig. 4a, bottom) shows a major content of calcium with atomic concentration reached 41.51%. Traces of chlorine (Cl, 1.20%) and sodium (Na, 0.44%) were detected in the sample, which confirm halite salts (NaCl). The mineralogical analysis using X-ray diffraction method measured calcite ( $\text{CaCO}_3$ , 85.90%) and halite (14.10%) (Fig. 5a). Limestone was a major building material used in constructing several Islamic structures in Cairo. The stone blocks were provided from the nearby quarries, e.g. El-Mokattam quarry (Harrell and Storemyr,

2009). The amounts of sodium chloride detected in the stone samples have two possible sources. First, halite is occurred as a natural impurity in sedimentary rocks (Nazel, 2016). Second, the impact of ground water level which affects many monuments at historic Cairo (Aly and Hamed, 2020). Actually, a notable effect was reported due to the Quaternary water layer, resulting from industrial and agricultural activities, in the North East of Cairo (Coppola et al., 2020). Seriously, water capillary penetration beneath the matrix will produce a severe damage (Ababneh, 2015).

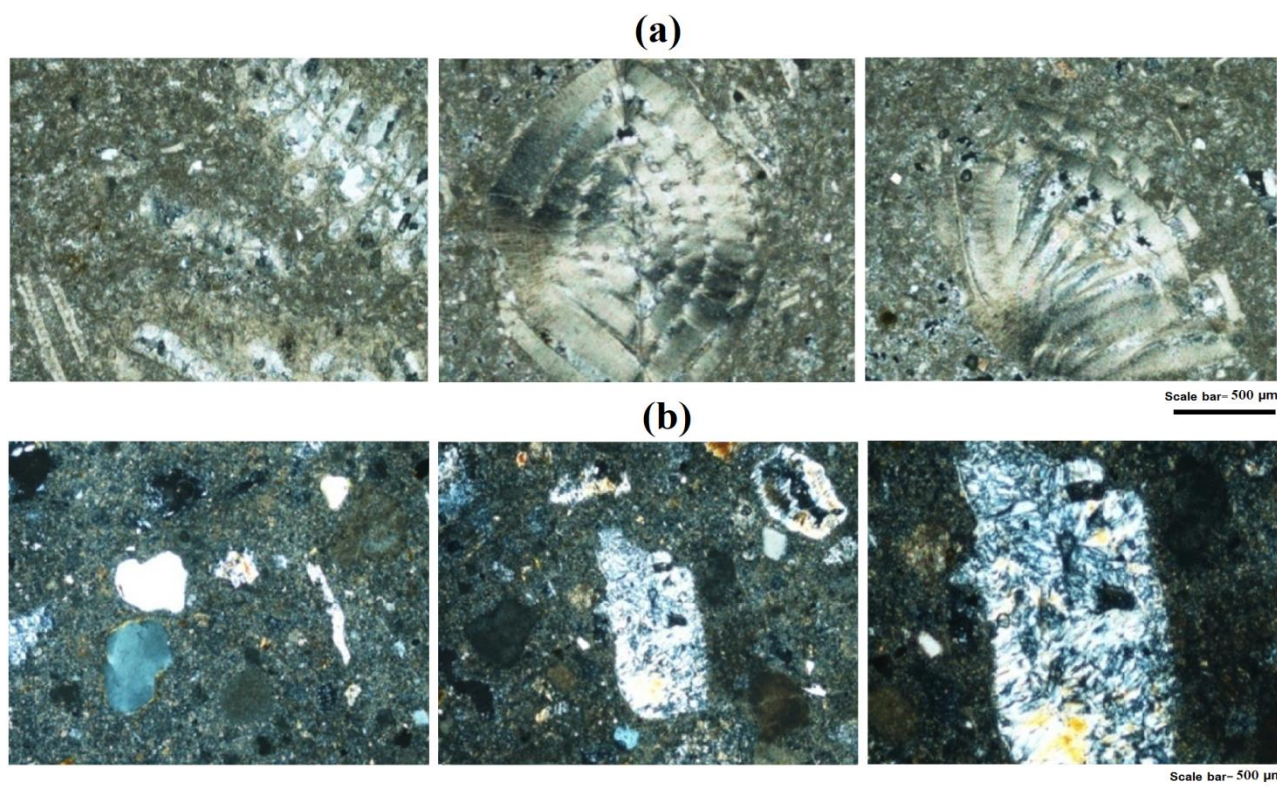


Figure 3. Crossed polarized light images (scale bar= 500  $\mu\text{m}$ ) of: a) stone sample, b) render layer.

### 3.2. Render layer

The petrographic examination on render layers represented fine calcite crystals with quartz grains of slightly small size (Fig. 3b). FE-SEM micrograph on the sample represented fine-grained matrix with the absence of siliceous aggregates (Fig. 4b). EDAX analysis confirmed high percentage of calcium (37.18 %) (Fig. 4b, bottom). Minor concentrations of sulfur (S, 2.85%), chlorine (1.60%) and sodium (0.69%) come from accumulations of halite and calcium sulfate phases. XRD diffractogram of the powder sample resulted in form of calcite (93.8%) with few quantity of quartz (6.20%) (Fig. 5b). The results are in accordance with the microscopic examination which expressed the high amount of calcite in the render layer compared to the siliceous aggregates. Probably, a siliceous limestone type was burned to prepare the lime. Technically, lime is produced through burning limestone blocks, often at temperatures of 920-1000°C. But also, calcium oxide (CaO) can be obtained in reducing conditions at temperature  $\sim 850^\circ\text{C}$  (Rodríguez-Navarro et al., 2009). After that, the heated blocks are crushed to fine powder of quick lime, which then is slaked with water to form calcium hydroxide,

Ca(OH)<sub>2</sub> (Artioli, Secco and Addis, 2019). After drying, Ca(OH)<sub>2</sub> transforms into calcite by carbonization (Liritzis et al., 2015). However lime was common to create fresco paintings, an exceptional use of dolomite powder was reported in 16th -17th century fresco at the Sviyazhsk Assumption Cathedral, Russia (Khramchenkova et al., 2018). In fresco technique, the wet lime putty reacts with the surrounding CO<sub>2</sub> gas to form a solid layer of calcium carbonate.

One of the main features of fresco is that the pigment particles are distributed into the carbonate layer, which enhances its durability as a painting technique. Amounts of sulfur (S) were reported through the EDAX analysis of the render layer, which refer to sulfate minerals (e.g. gypsum, CaSO<sub>4</sub>·2H<sub>2</sub>O). Probably, the absence of gypsum in the XRD pattern is due to that its amount was below the detection limit of the instrument. Gypsum is formed as a result of chemical deterioration, in this process, calcite crystals are replaced by sulfate crystals (gypsum) through the sulphation process (Benedetti et al., 2007). The origin of sulfates may originate from external sources, e.g. atmospheric pollution or from the groundwater rising in the studied area.

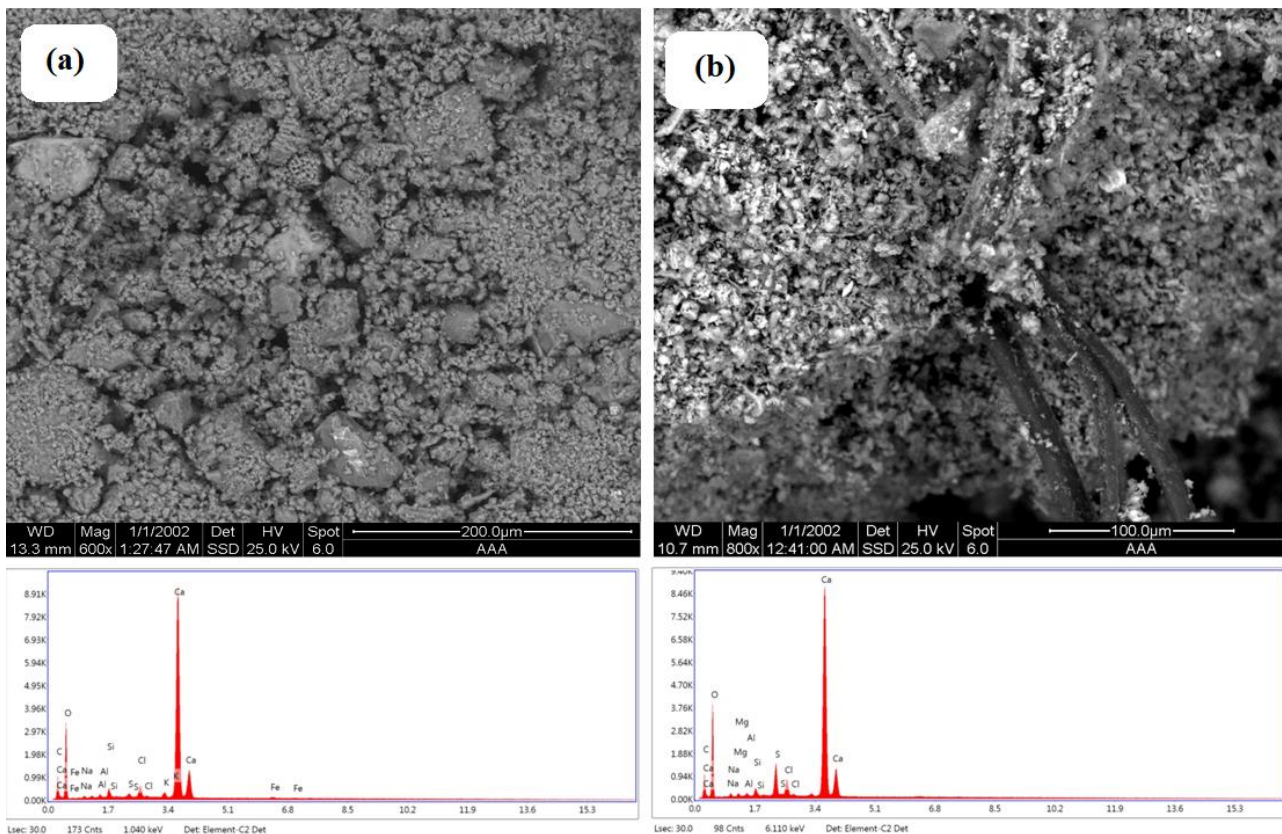


Figure 4. FE-SEM micrographs and EDAX spectra of: a) stone sample, b) render sample.

### 3.3. Paint layers

#### 3.3.1. Blue paint layer

The FE-SEM image scanned on the blue paint layer showed a homogenous distribution of fine grains (Fig. 6a). The EDAX spectrum (Fig. 6b) measured concentrations of sodium (Na, 0.58%), aluminum (Al, 0.76%), sulfur (S, 6.06), chlorine (Cl, 0.80%), and silicon (Si, 0.79). These characteristic elements suggest the application of ultramarine blue. The microscopic image presented in Figure 6b, shows deep blue grains of the pigment material. The mineralogical analysis, by XRD, showed the existence of lazurite (Na, Ca)<sub>8</sub>(AlSiO<sub>4</sub>)<sub>6</sub>(SO<sub>4</sub>S,Cl)<sub>2</sub> (Fig. 6c). The mineral lazurite forms the majority of the precious stone 'Lapis lazuli'. Lapis lazuli was used since pre-dynastic but its powder 'the ultramarine blue' likely was first used by the 5th and 8th centuries C. E. Ultramarine blue contains particles with size larger than >10 μm (Aceto et al., 2013). In the FTIR analysis of the sample, compared with standard spectra of animal glue and gum Arabic (Fig. 6d), recognizable bands of calcite and gypsum together with stretching vibration of S-S bond near 546 cm<sup>-1</sup>, correspond to lazurite, were identified (Bruni et al., 1999). Worthy to note that no organic material was identified, which ascertains the use of

fresco technique. Fresco technique is a durable technique due to the absence of organic materials in the structure and the antimicrobial effect of lime (Vázquez de Ágredos-Pascual et al., 2019).

#### 3.3.2. Orange-red paint layer

The investigation of the red-orange paint sample by FE-SEM (Fig. 7a) showed a bright shiny surface which reflects the presence of heavy metals. Observing the EDAX spectrum, a high concentration of lead (Pb, 24.40%) (Fig. 7b) was measured. XRD pattern of the sample (Fig. 7c) showed minium (Pb<sub>3</sub>O<sub>4</sub>) as the coloring mineral in the sample. However red ochre was the principal coloring agent used in many chronological periods, but some other pigments such as realgar (As<sub>4</sub>S<sub>4</sub>) and red lead were used for red-orange hue. Red lead was a pioneer artificial pigment used for painting and it was reported in China by the 5th century BC. (Miguel et al., 2009). This pigment can be simply produced by the calcinations of basic lead carbonate (2PbCO<sub>3</sub>·Pb(OH)<sub>2</sub>), and also by the oxidation of litharge (Lead monoxide) (Aze et al., 2008). The size of particles ranges between 1 to 50 micron. Despite its vivid color, red lead transforms into black lead dioxide, by the effect of sulfuric gases. In their study of the discoloration phenomenon of mural paintings of Mogao Grottoes (366 AD), Zhao et al. (2016) realized

that the degradation of red lead pigment is linked to the humid microclimate and the microbiological effects with a fluent supply of  $H^+$  ions. In Figure 7d, the FTIR spectra of the red-orange paint layer, animal

glue, and gum Arabic are presented. In infrared spectra, lead oxide usually gives a collection of absorption bands near  $680$  and  $520\text{ cm}^{-1}$  (Čiuladienė et al., 2018).

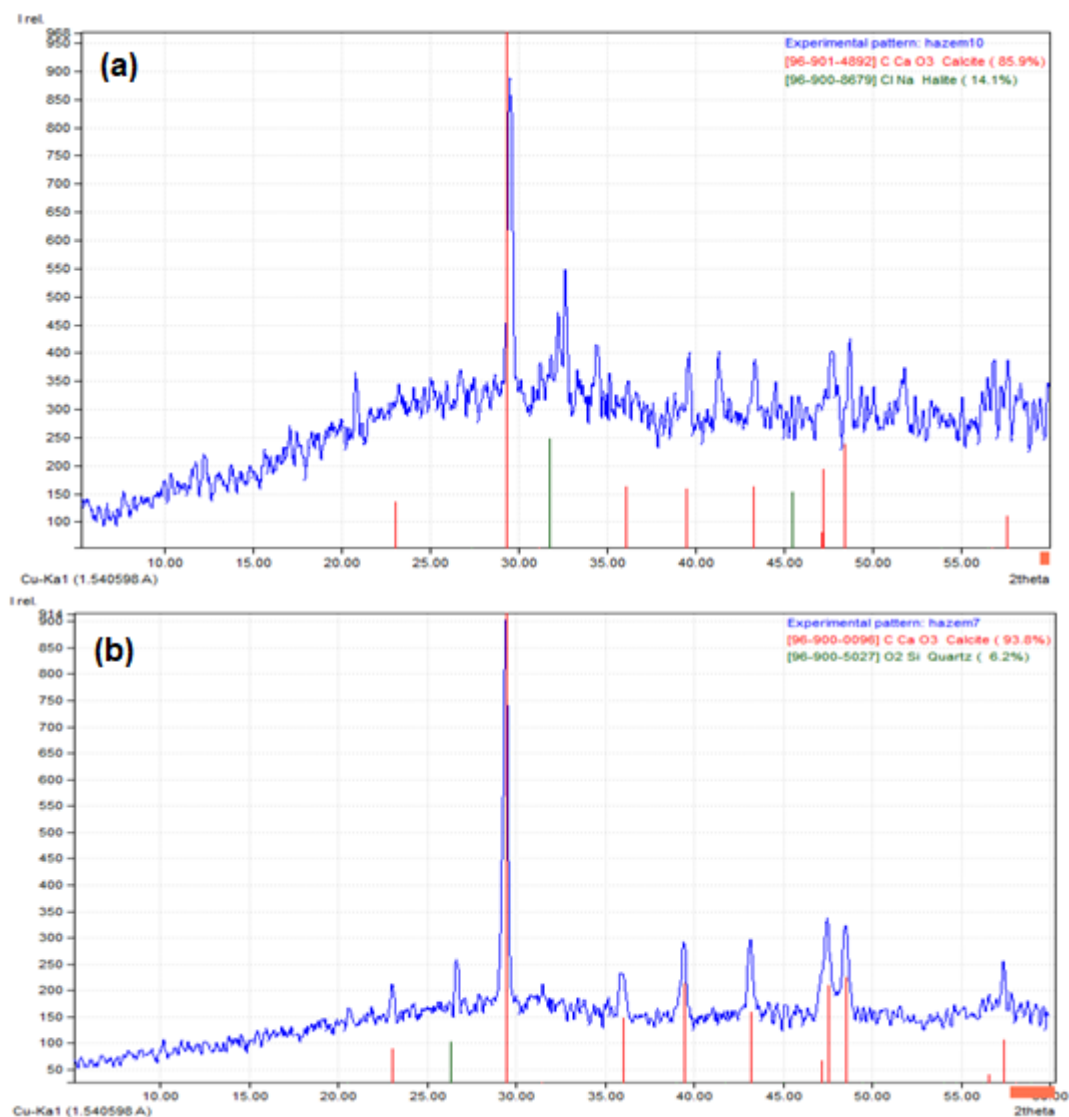


Figure 5. XRD diffractograms recorded on: a) powder stone sample, b) powder render sample.

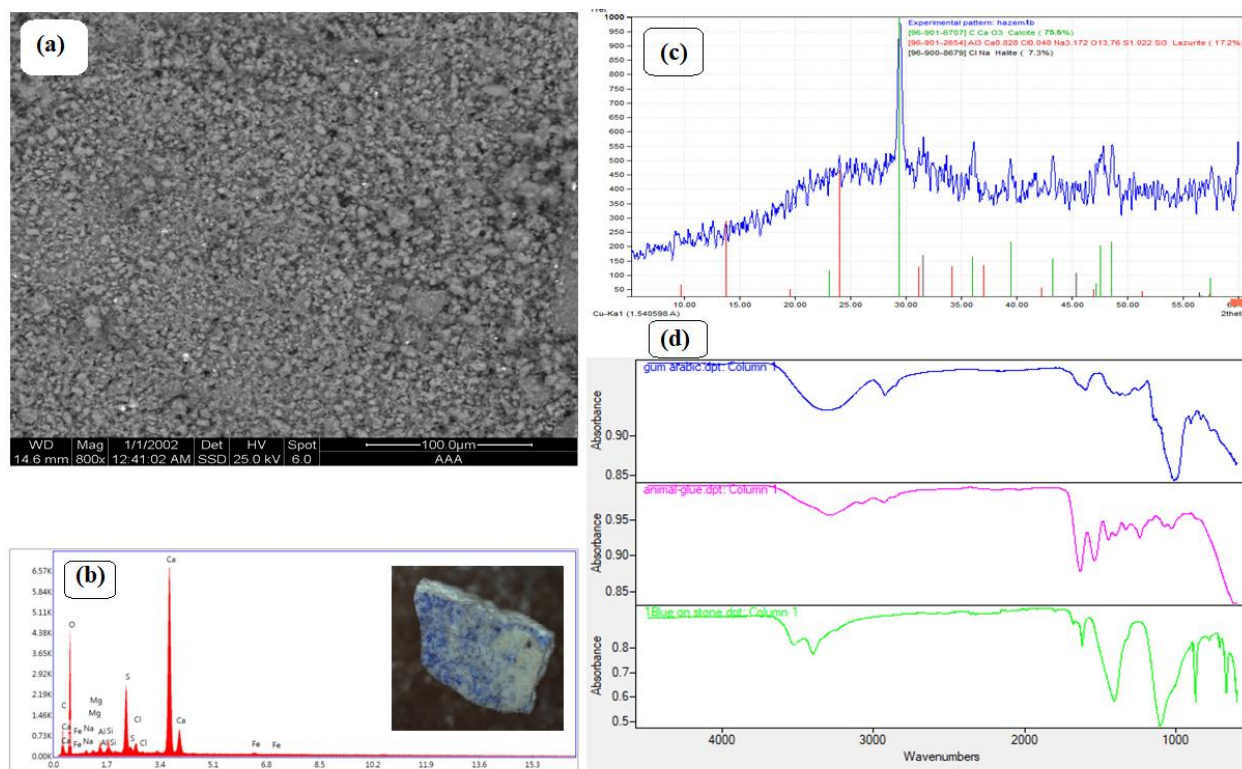


Figure 6. a) FE-SEM image of the blue paint layer, b) EDAX spectrum of the sample (a microscopic image is also presented), c) XRD diffractogram of the sample, d) FTIR spectra on the sample compared with standards of animal glue and gum Arabic.

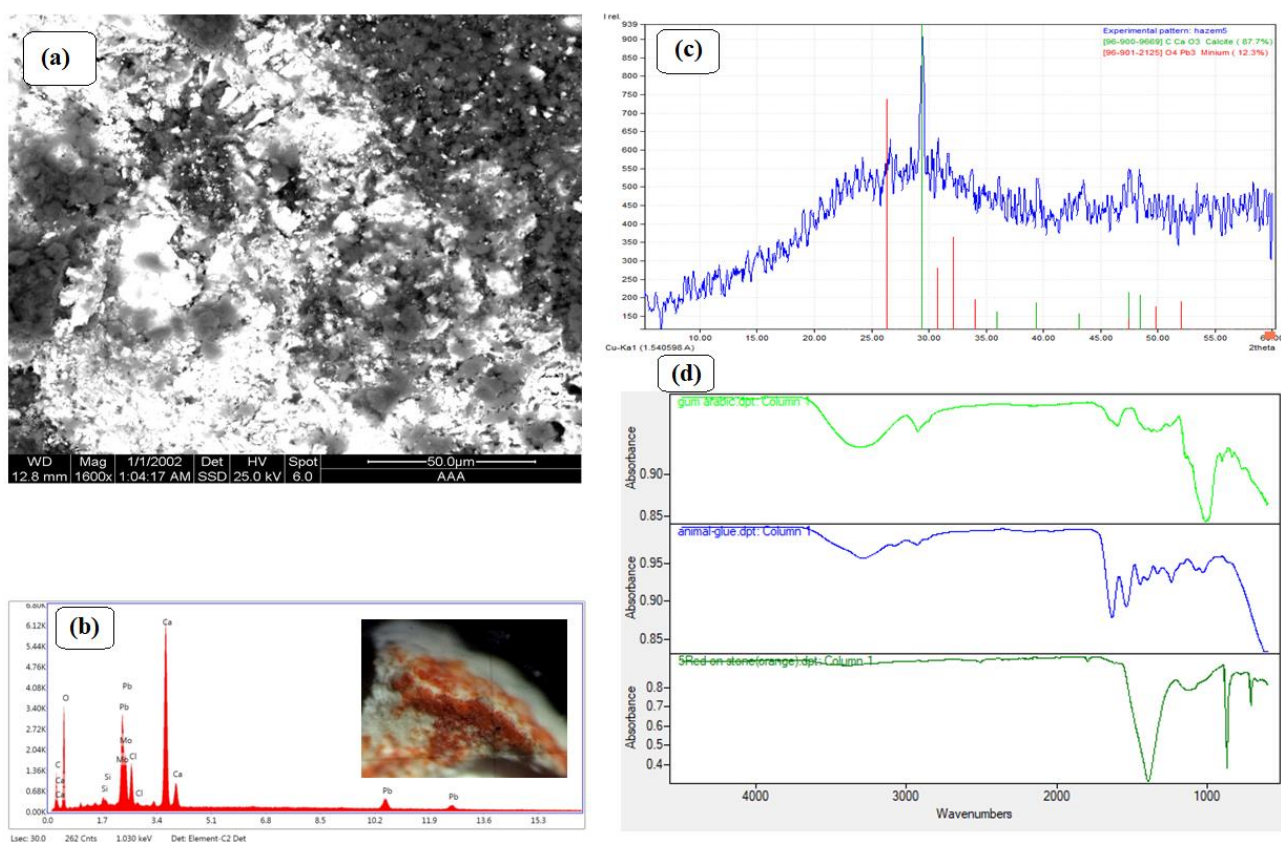


Figure 7. a) FE-SEM image of the orange-red paint layer, b) EDAX spectrum of the sample (a microscopic image is also presented), c) XRD diffractogram of the sample, d) FTIR spectra on the sample compared with standards of animal glue and gum Arabic.

### 3.3.3. Green paint layer

Analysis of the green paint layer showed interesting results. The morphology of the sample revealed coarse large grains together with bright crystals (Fig. 8a, up). The EDAX spectrum measured a wide group of elements including two featured elements, arsenic (As, 5.83%) and copper (Cu, 3.88%) (Fig. 8a, bottom). It seems that the ancient artist decided to create the green hue through mixing different pigments. Probably, a mixture of azurite ( $\text{Cu}_3(\text{CO}_3)_2(\text{OH})_2$ ) and arsenic-based yellow pigment (e.g. orpiment) was used. According to Lucas (1962), azurite probably was used as a pigment since the 4th Dynasty in Egypt (c. 2613-2494 BC). However, no strong indication was reported to support this argument. In his review article, Scott (2016) claimed that some researchers found azurite on different objects. Orpiment, as a royal pigment, was a brilliant yellow pigment imported to

Egypt since the 18th Dynasty (1549-1292 BC) (El Goresy et al., 1986).

### 3.3.4. Pink paint layer

For the pink paint layer, the FE-SEM image showed the grains of the pigment appeared fine with large ones of quartz (Fig. 8b, up). EDAX analysis measured calcium (31%) with few amounts of iron (3.14%) (Fig. 8b, bottom). Complementary concentrations of sulfur (5.12%) and silicon (1.93%) were found. The pink hue probably was produced by mixing portions of red hematite ( $\text{Fe}_2\text{O}_3$ ), gypsum and calcite. The amounts of silicon refer to quartz, while the absence of aluminum (Al) suggests that hematite rather than ochre was used. Hematite has a wide range of hues, of them, red-orange, red and bright red were the widely used throughout history (Marey Mahmoud, 2011).

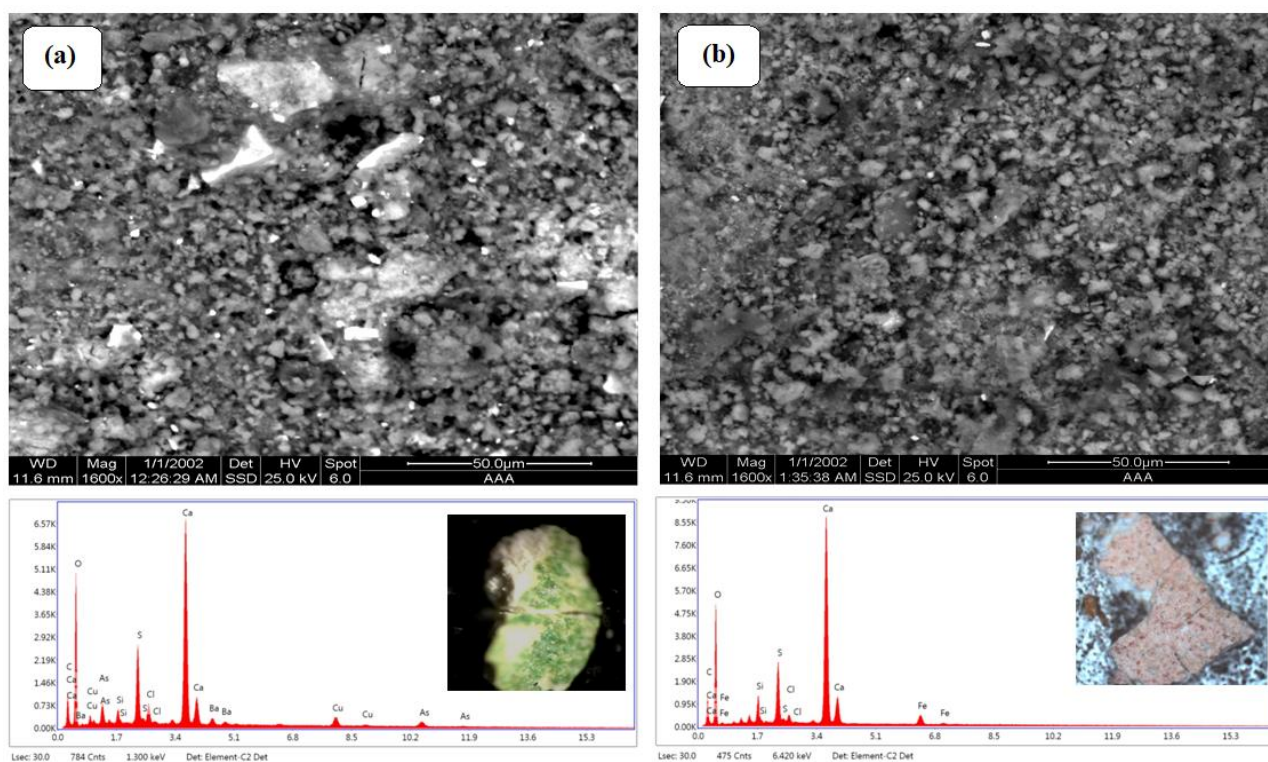


Figure 8. a) FE-SEM image (up) and EDAX spectrum (bottom) of the green paint layer, b) FE-SEM image (up) and EDAX spectrum (bottom) of the pink paint layer.

### 3.3.5. Black paint layer

No characteristic features were documented for the black paint layer. The morphology of the pigment (Fig. 9, right side) excludes the use of charred char-

coal. Also, the microanalysis did not detect phosphorus in the sample. It was concluded that lampblack was used to produce the black color. Lampblack is one of the oldest known carbon pigments. It has fine particles that usually collected from soot results from oil lamps (Lliveras-Tenorio et al., 2019)

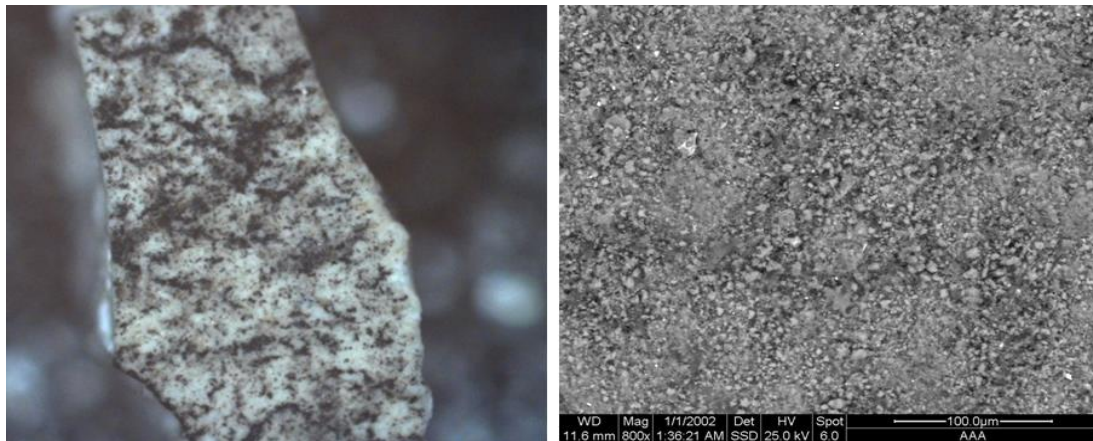


Figure 9. A microscopic image of the black paint layer (left) and FE-SEM image shows the fine particles of the pigment (right).

### 3.4. Restoration procedures

*In-situ* observations and analysis of the historical records helped to conclude that the mural was added to the original structure at later era (probably in the Ottoman period). The mural shows a niche painting presents an arch intertwined with plant motifs and half-circles, hanging from them shapes and means of lighting (e.g. lamps). This niche is surrounded with floral motifs and longitudinal lines and triangles interchangeably, perhaps symbolizing domes. The mu-

ral was photographically recorded, as the photographic documentation is one of the most important steps in the restoration work. Figures 10 & 11 represent photographic and drawing documentation of the main deterioration forms recorded on the mural. It was easy to record that the mural can hardly be seen due to fading occurred by the effect of time. Accumulations of recent lime layers, salts efflorescence, missing painted areas, several cracks and disintegration of the pictorial surface were observed. After fluffing the necessary documentations, several restoration steps were applied (Fig. 13).

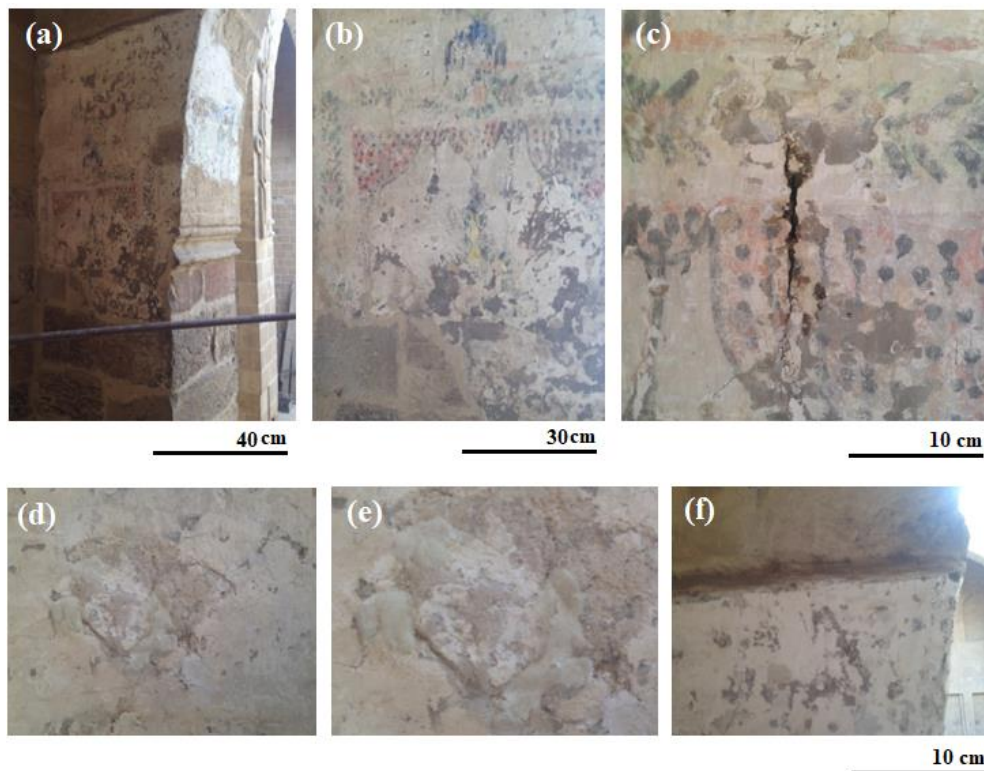


Figure 10. Photographic documentation of the studied mural, a) disfiguring of the mural, b) a close-up image of the previous image, c) crack, d-f) recent lime layers on the mural.

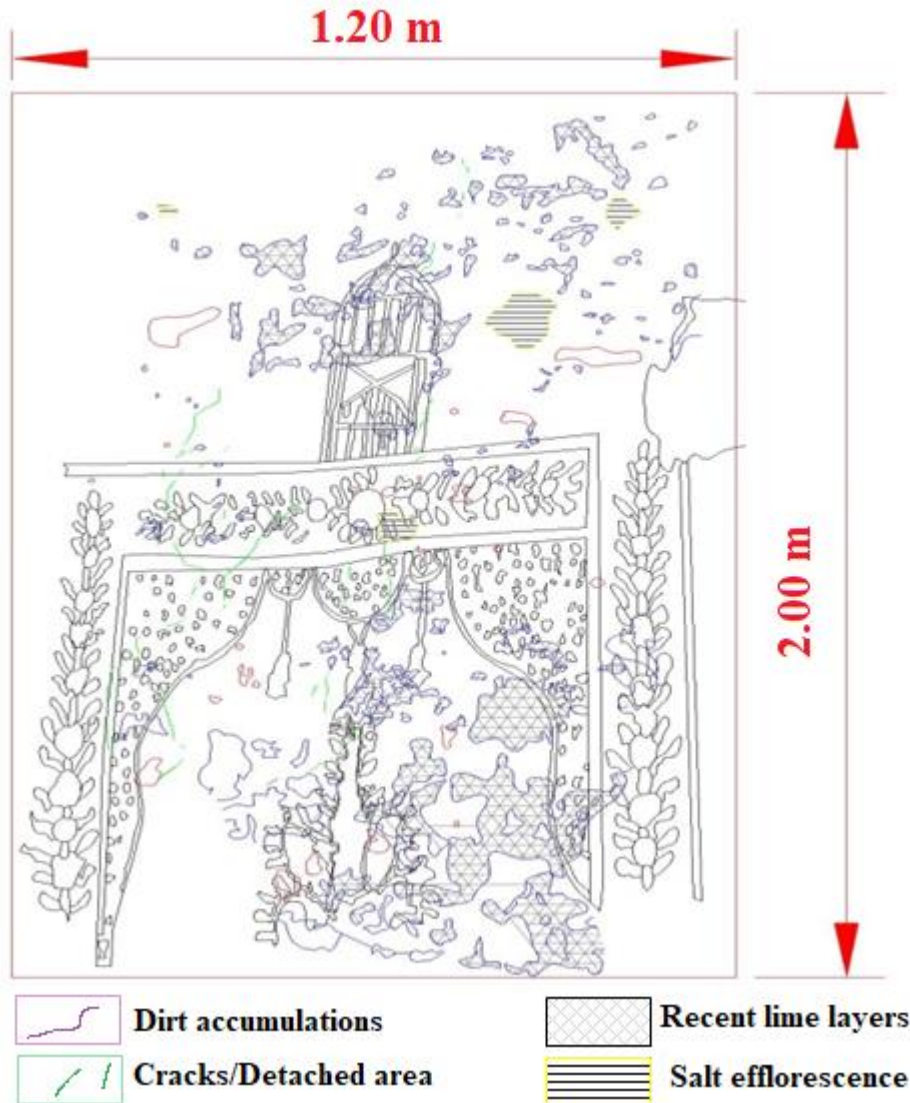


Figure 11. A map illustrating the main deterioration aspects on the mural.

### 3.4.1. Primary stabilization

Before starting restoration work, a visual examination was necessary to identify the weak areas that exist in the mural as a result of the exposure to external weathering factors. First aid has been carried out to preserve and maintain the mural. An acrylic emulsion of Primal AC-33 (20% in water) was used to stabilize the weak layers and to enhance their cohesion before proceeding the restoration.

### 3.4.2. Mechanical Cleaning

In any restoration project, the mechanical cleaning usually comes first to remove any undesired accumulations. This method is highly controlled and preferable to minimize the need for further chemical methods. The mechanical cleaning was done from top to bottom. The hand blower and soft and coarse brushes of various shapes and sizes were used to remove dirt

and dust from the surface as well as using scalpels to remove the recent lime layers and salt crystals.

### 3.4.3. Chemical Cleaning

When no enough results are obtained through mechanical tools, chemical cleaning is applied. To facilitate the removal of adhered dirt layers, paper pulp poultice with water, alcohol and neutral soap (2:1:1) was applied onto the surface. Then, the poultice was covered with polyethylene sheet, then the layers were removed mechanically.

### 3.4.4. Cracks repair and injecting detached layers

The open cracks were cleaned well with an air blower and the dust accumulations were cleaned with water and ethyl alcohol to ensure a good adhesion for the repair mortar. A repair mortar consists of washed

sand, lime, Primal-33 and Wacker OH100 was injected into the voids of cracks. The mortar grout was applied with intervals to ensure a good penetration into the mural structure. For some detached paint layers, drops of Primal AC-33 (20%) were applied by syringes with the aid of gentle pressing on the separate parts to return them back to their original places.

### 3.4.5. Consolidation

Consolidation is usually applied as a final step to provide long-term strengthening and protection against the surrounding atmospheric conditions. Several polymeric materials are used for this purpose but for the last decades, nanomaterials have been used successfully. Based on experimental approaches, a

dispersion of Nanolime (nano  $\text{Ca}(\text{OH})_2$ ), 5% dispersed in ethyl alcohol, was applied, for several times with an interval of a week after each application, using the brushing method. The surface was covered with polyethylene sheets to prevent the rapid evaporation of the alcohol. The scanning electron microscope was used to evaluate the consolidation process and stability of the nanomaterials against weathering factors. In Figure 12, the appearance of the prepared nano dispersion was evaluated by FE-SEM investigation after laboratory salt weathering. In the FE-SEM image, one can notice the high stability of the new formed crystals of calcium carbonate against etching that usually occurred due to crystallization of salts as previously reported by Al-Omary et al., (2018).

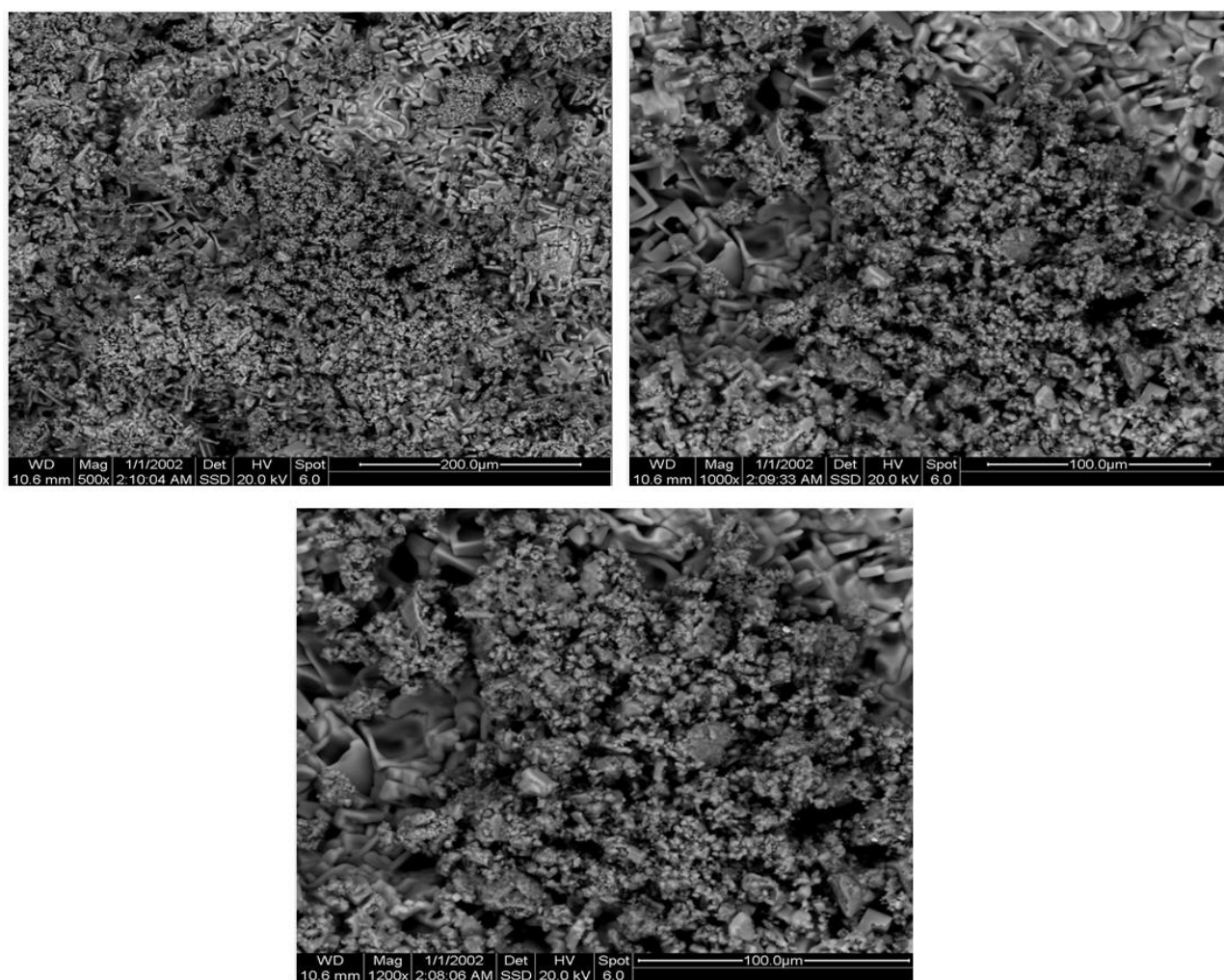


Figure 12. FE-SEM micrographs (at magnifications 500, 1000 and 1200x) of the treated paint layer with nanolime (5% in ethyl alcohol) after laboratory salt weathering.



Figure 13. a) examples of the restoration procedures applied to the murals (e.g. cleaning, injection of open cracks, etc), b) the studied mural after the final steps of restoration (the yellow arrow refers to location of the mural).

#### 4. CONCLUSION

A surviving mural painting on the walls of Al-Bimāristān Al-Mu'ayyidi, a featured Mumluk monument at Cairo the building, was studied and preserved. A number of widely used analytical methods helped to characterize the microscopic and petrographic features of the samples. Besides, the morphological and microanalysis together with mineralogical structure were determined. The results revealed calcite as the main component of the stone support, while halite was the dominant salt type affects in the site. The render layer was analyzed as calcium carbonate (calcite) with few amount of quartz. Pigments

of lazurite 'Lapis Lazuli', red lead (minium), hematite, azurite and yellow orpiment were identified. Since calcite was used for the render layer and FTIR detected no organic matter, it was concluded that 'fresco' technique was used. The studied monument, as the case of many buildings in historic Cairo, suffered severe deterioration factors which affected badly the examined mural. For this, a restoration project of cleaning, injecting detached layers, cracks repair and consolidation was necessary. Further, the efficiency of nanolime dispersion in strengthening the carbonate-based matrix was confirmed. The results of this study showed the high-priority to document the remains of Islamic mural paintings in the heritage buildings of Egypt.

## REFERENCES

- Ababneh, A. (2015) Qusair Amra (Jordan) world heritage site: a review of current status of presentation and protection approaches. *Mediterranean Archaeology and Archaeometry*, 15(2), pp. 27–44.
- Abdel Alim, F. (2003) *Islamic Architecture in Mumluk (time of Sultan Al-Mu'ayyidi)*, In Arabic. The 100 book project, Supreme Council of Antiquities, Cairo.
- Aceto, M., Agostino, A., Fenoglio, G. and Picollo, M. (2013) Non-invasive differentiation between natural and synthetic ultramarine blue pigments by means of 250–900 nm FORS analysis. *Analytical Methods*, 5, 4184.
- Ali, M.F. and Abd Elkawy, M.H. (2021) Physical analysis and treatment of disintegrated Islamic mural paintings from the 15th century Taqi Aldin Albistami hospice. *SCIENTIFIC CULTURE*, 7(1), pp. 45–56.
- Al-Omary, R.A., Al-Naddaf, M. and Al Sekhaneh, W. (2018) Laboratory evaluation of Nanolime consolidation of limestone structures in the Roman site of Jerash, Jordan. *Mediterranean Archaeology and Archaeometry*, 18(3), pp. 35–43.
- Aly, H. and Hamed, A. (2020) The impact of salt crystallization on the building stones of Al-Azhar mosque from historic Cairo – Egypt. *International Journal of Conservation Science*, 11(4), pp. 895–904.
- Artioli, G., Secco, M. and Addis, A. (2019) The Vitruvian legacy: mortars and binders before and after the Roman world. *EMU Notes in Mineralogy*, 20, pp. 151–202.
- Aze, S., Vallet, J.-M., Detalle, V., Grauby, O. and Baronnet, A. (2008) Chromatic alterations of red lead pigments in artworks: a review. *Phase Transitions*, 81(2), pp. 145–154.
- Behrens-Abouseif, D. (2007) *Cairo of the Mamluks. A History of the Architecture and its Culture*. The American University in Cairo Press.
- Benedetti, D., Bontempi, E., Pedrazzani, R., Zacco, A. and Depero, L. E. (2007) Transformation in calcium carbonate stones: some examples. *Phase Transitions*, 81(2), pp. 155–178.
- Bianchin, S., Casellato, U., Favaro, M. and Vigato, P.A. (2007) Painting technique and state of conservation of wall paintings at Qusayr Amra, Amman e Jordan. *Journal of Cultural Heritage*, 8, pp. 289–293.
- Bruni, S., Cariati, F., Casadio, F. and Toniolo, L. (1999) Spectrochemical characterization by micro-FTIR spectroscopy of blue pigments in different polychrome works of art. *Vibrational Spectroscopy*, 20, pp. 15–25.
- Čiuladienė, A., Luckutė, A., Kiuberis, J. and Kareiva, A. (2018) Investigation of the chemical composition of red pigments and binding media. *CHEMIJA*, 29(4), pp. 243–256.
- Coppola, M., Di Benedetto, F., Garzonio, C.A., Pecchioni, E. and Santo, A.P. (2020) Groundwater damages on the historic buildings of Cairo: the case of the medieval walls of Mokattam limestone. *IOP Conference Series: Materials Science and Engineering*, 949, 012004.
- El Goresy, A., Jaksch, H., Abdel Razek, M. and Weiner, K.L. (1986) *Ancient pigments in wall paintings of Egyptian tombs and temples: an archaeometric project*. In: Trenkwalder, H., Purtscheller, F., Lukas, W. and Seidl, H. (Eds.), *Interdisziplinäres Gespräch: Geisteswissenschaft-Naturwissenschaft- Technik anhand konkreter Projekte*. Sonderheft des Bundesministerium für Wissenschaft und Forschung, Wien, pp. 1–57.
- Fikri, I., El Amraoui, M., Haddad, M., Ettahiri, A.S., Bellot-Gurlet, L., Falguères, C., Lebon, M., Nespoulet, R., Ait Lyazidi, S. and Bejjit, L. (2018) XRF and UV-Vis-NIR analyses of medieval wall paintings of al-Qarawiyyin Mosque (Morocco). *IOP Conference Series: Materials Science and Engineering*, 353, 012020.
- Hampikian, N. (2012) Mu'ayyad Šayḥ and the Landscape of Power, *Annales Islamologiques*, 46, pp. 195–214.
- Harrell, J.A. and Storemyr, P. (2009) *Ancient Egyptian quarries – an illustrated overview*. In Abu-Jaber, N., Bloxam, E.G., Degryse, P. and Heldal, T. (eds.) *QuarryScapes: ancient stone quarry landscapes in the Eastern Mediterranean*, Geological Survey of Norway Special Publication, 12, pp. 7–50.
- Holt, P. M. (1993) *al-Mu'ayyad Shaykh*. *The Encyclopaedia of Islam*. Leiden.
- Gil-Torrano, A., Gómez-Morón, A., Martín, M. J., Ortiz, R., del Camino Fuertes Santos, M. and Ortiz, P. (2019) Characterization of Roman and Arabic Mural Paintings of the Archaeological Site of Cercadilla (Cordoba, Spain). *Scanning*, 2019, Article ID 3578083.
- Goldstein, J.I., Lyman, Ch, L., Newbury, D.E., Lifshin, E., Echlin, P., Sawyer, L., Joy, D.C. and Michael, J.R. (2007) *Scanning Electron Microscopy and X-Ray Microanalysis*. 3rd edition, Springer Science & Business Media, LLC.
- Khramchenkova, R., Biktagirova, I., Gareev, B. and Kaplan, P. (2018) Horse-headed saint Christopher fresco in the Sviyazhsk Assumption cathedral (16th -17th century, Russia): history and Archaeometry. *Mediterranean Archaeology and Archaeometry*, 18(3), pp. 195–207. DOI: 10.5281/zenodo.1476971

- Liritzis, I., Al-Otaibi, F., Kilikoglou, V., Perdikatsis, V., Polychroniadou, E. and Drivaliari, A. (2015) Mortar analysis of wall painting at Amfissa cathedral for conservation–restoration purposes. *Mediterranean Archaeology and Archaeometry*, 15(3), pp. 301-311. DOI: 10.5281/zenodo.33833
- Lluveras-tenorio, A., Spepi, A., Pieraccioni, M., Legnaioli, S., Lorenzetti, G., Palleschi, V., Vendrell, M., Colombini, M.P., Tinè, M.R., Duce, C. and Bonaduce, I. (2019) A multi-analytical characterization of artists' carbon-based black pigments. *Journal of Thermal Analysis and Calorimetry*, 138, pp. 3287–3299.
- Lucas, A. (1962) *Ancient Egyptian Materials and Industries*, Rev., Harris, J.R., Edward Arnold Publ., Ltd., 4th Ed., London.
- Mahmoud, H.S.A. (2021) Multiscientific approach for the characterization and assessment of the degradation state of the historical Al-Shafi'i mosque walls (Jeddah, Kingdom of Saudi Arabia). *SCIENTIFIC CULTURE*, 7(1), pp. 1–19.
- Marey Mahmoud, H. (2011) A preliminary investigation of ancient pigments from the mortuary temple of Seti I, El-Qurna (Luxor, Egypt). *Mediterranean Archaeology and Archaeometry*, 11(1), pp. 99–106.
- Miguel, C., Claro, A., Pereira Gonçalves, A., Muralha, V. S. F. and Melo, M.J. (2009) A study on red lead degradation in a medieval manuscript Lorvão~ Apocalypse (1189). *Journal of Raman Spectroscopy*, 40, pp. 1966–1973.
- Nazel, T. (2016) The Sharaf Al-Din Mosque in Cairo: A Case Study. *Restoration of Buildings and Monuments*, 22, pp. 27–36.
- Rodriguez-Navarro, C., Ruiz-Agudo, E., Luque, A., Rodriguez-Navarro, A.B. and Ortega-Huertas, M. (2009) Thermal decomposition of calcite: mechanisms of formation and textural evolution of CaO nanocrystals. *American Mineralogist*, 94, 578593.
- Scott, D.A. (2016) Review article A review of ancient Egyptian pigments and cosmetics. *Studies in Conservation*, 61(4), pp. 185–202.
- Vázquez de Ágredos-Pascual, M.L., Zapata-Meza, M., Sanz-Rincón, R., Garza DíazBarriga, A., Expósito De Vicente, C., Rojo-Iranzo, L. and Herreras Sala, S. (2019) Physicochemical and cultural study of coloring materials from 1st c. AD Magdala, Lower Galilee. *Mediterranean Archaeology and Archaeometry*, 19(3), pp. 173-188. DOI: 10.5281/zenodo.3583077.
- Yeomans, R (2006) *The art and architecture of Islamic Cairo*, Garnet Publishing Limited, UK.
- Zhao, Y., Tang, Y., Tong, T., Sun, Z., Yu, Z., Zhud, Y. and Tong, H. (2016) Red lead degradation: monitoring of color change over time. *New Journal of Chemistry*, 40, pp. 3686–3692.